SUPPLEMENTAL DATA

Sex-dependent effects of chromogranin B P413L allelic variant as a disease modifier in amyotrophic lateral sclerosis

Yasuyuki Ohta, Genevieve Soucy, Daniel Phaneuf, Jean-Nicolas Audet, François Gros-Louis, Guy A. Rouleau, Hélène Blaco, Philippe Corcia, Peter M. Andersen, Frida Nordin, Toru Yamashita, Koji Abe and Jean-Pierre Julien

SUPPLEMENTARY FIGURE LEGENDS

Figure S1. Defective binding of CHGB^{P413L} variants to mutant SOD1 and interaction of mouse CgB with mutant SOD1 and misfolded SOD1 *in vitro*. (A) Defective interaction of genomic CHGB^{P413L} variant with mutant SOD1^{G93A} in cultured cells. Neuro2A cells were co-transfected with FLAG-SOD1^{G93A} and genomic CHGB. IP-FLAG fractionated by two-dimensional gel electrophoresis. (B, C) Partial co-localization of mutant SOD1^{G93A} and misfolded SOD1 (misfSOD1) with mCgB in cultured cells. Neuro2a cells were transfected with FLAG-SOD1 and HA-mCgB. Immunostained cells using anti-HA and anti-FLAG (B) or anti-misfSOD1 (B8H10) antibodies (C) were observed by confocal microscopy. Arrowheads indicate CgB accumulation and SOD1^{G93A} (B) or misfSOD1 (C) merged with CgB. Scale bars, 10 μm.

Figure S2. Neurite outgrowth impairment of CHGB^{P413L} and CHGB^{H230R} variants *in vitro*. Neuro2A cells were transfected with HA-tagged CHGB. Immunostained cells using anti-HA and anti-actin antibodies were observed by confocal microscopy. The percentage of cells expressing neuritis (arrow heads), the average number of neurites per cell, and the average length of neuritis were analyzed. Bars show $p<0.05$ in

post-ANOVA Turkey test. Scale bars, 10 μm.

Figure S3. Accelerated disease onset in $SOD1^{G37R}$ mice overexpressing $CHGB^{L413}$ transgene. (A) Overexpression of $CHGB^{P413}$ or $CHGB^{L413}$ proteins in the microsomal fractions of the spinal cords of mice. Subcellular fractions of mice (210 days of age) were analyzed by immunoblotting. NTg, non-transgenic mice. (B) Accelerated disease onset in $SOD1^{G37R}$;$CHGB^{L413}$ mice. (C) Accelerated disease progression in $SOD1^{G37R}$;$CHGB^{P413}$ mice but not in $SOD1^{G37R}$;$CHGB^{L413}$ mice. Kaplan-Meier survival analysis and the log-rank test were used (B, C). (D) Increased ALS disease duration in $SOD1^{G37R}$;$CHGB^{L413}$ mice. Post-ANOVA Turkey test was used. (E, F) The decline of motor performance on rotarod test (E) and of body weight (F) at late stage of disease due to overexpression of $CHGB^{P413}$ in $SOD1^{G37R}$ mice. Data are mean ± SEM. $^{!}p<0.05$, $^{!!}p<0.01$ between $SOD1^{G37R}$ and $SOD1^{G37R}$;$CHGB^{P413}$, $^{\$}P<0.05$, $^{\$\$}p<0.01$ between $SOD1^{G37R}$;$CHGB^{P413}$ and $SOD1^{G37R}$;$CHGB^{L413}$ in post-ANOVA Turkey test.

Figure S4. No evidence of enhanced astrogliosis due to expression of either $CHGB^{P413}$ or $CHGB^{L413}$ in $SOD1^{G37R}$ mice at end stage. Signal intensities of GFAP in five lumbar cord sections from each mice (N=3-4) was analyzed. The values (mean ±SEM)

represent the ratio compared to control (G37R mice). Post-ANOVA Turkey test was used in each sex.

Figure S5. Gender differences of CHGB and SRY expression in the spinal cords of mice. (A) Higher expressions of CHGB proteins in female mice compared to males. Densitometry of CHGB in cytosolic/microsomal fractions of spinal cords were analyzed (Figure 5E). The values (mean ±SEM, N=3) representing the ratio compared to males. (B) The antisense probe for CHGB mRNA did not interact with endogenous mCgB mRNA. The lumbar cords of NTg female mice was analyzed by *in situ* hybridization. (C) SRY expression in the neurons of spinal cords of NTg male mice but not in females. Scale bars, 50 μm.

Fig S1

A

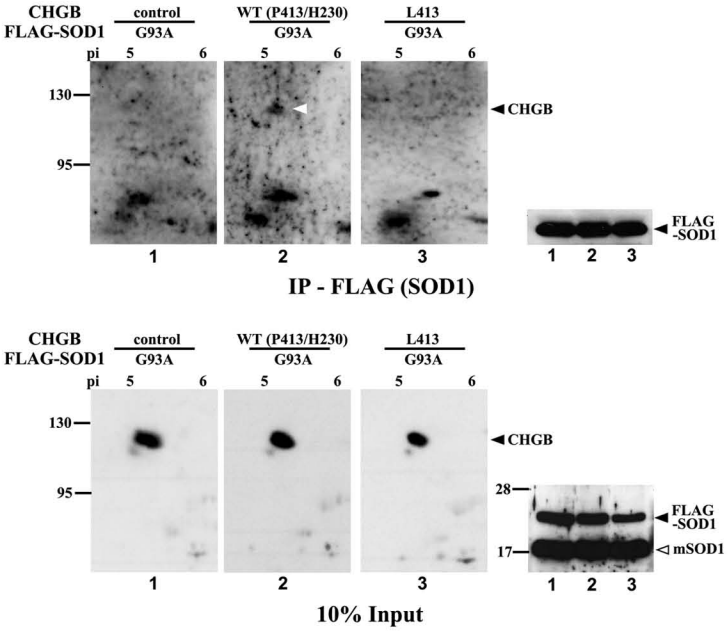
CHGB
FLAG-SOD1
control
G93A
WT (P413/H230)
G93A
L413
G93A
pi 5 6
5 6
5 6
130
95
CHGB
FLAG
-SOD1
1 2 3
1 2 3
IP - FLAG (SOD1)
CHGB
FLAG-SOD1
control
G93A
WT (P413/H230)
G93A
L413
G93A
pi 5 6
5 6
5 6
130
95
28
17
CHGB
FLAG
-SOD1
mSOD1
1 2 3
1 2 3
10% Input

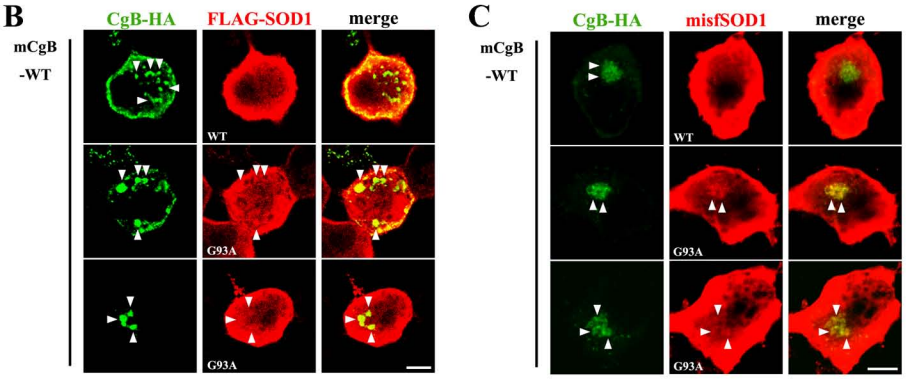
B
CgB-HA
FLAG-SOD1
merge
mCgB
-WT
WT
G93A
G93A
C
CgB-HA
misfSOD1
merge
mCgB
-WT
WT
G93A
G93A

Fig S2

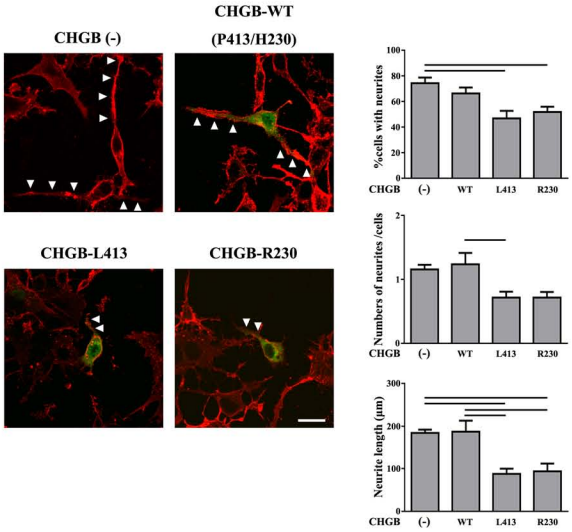
CHGB (-)
CHGB-WT
(P413/H230)
CHGB-L413
CHGB-R230
%cells with neurites
Numbers of neurites /cells
Neurite length (μm)
CHGB
(-)
WT
L413
R230

Fig S3

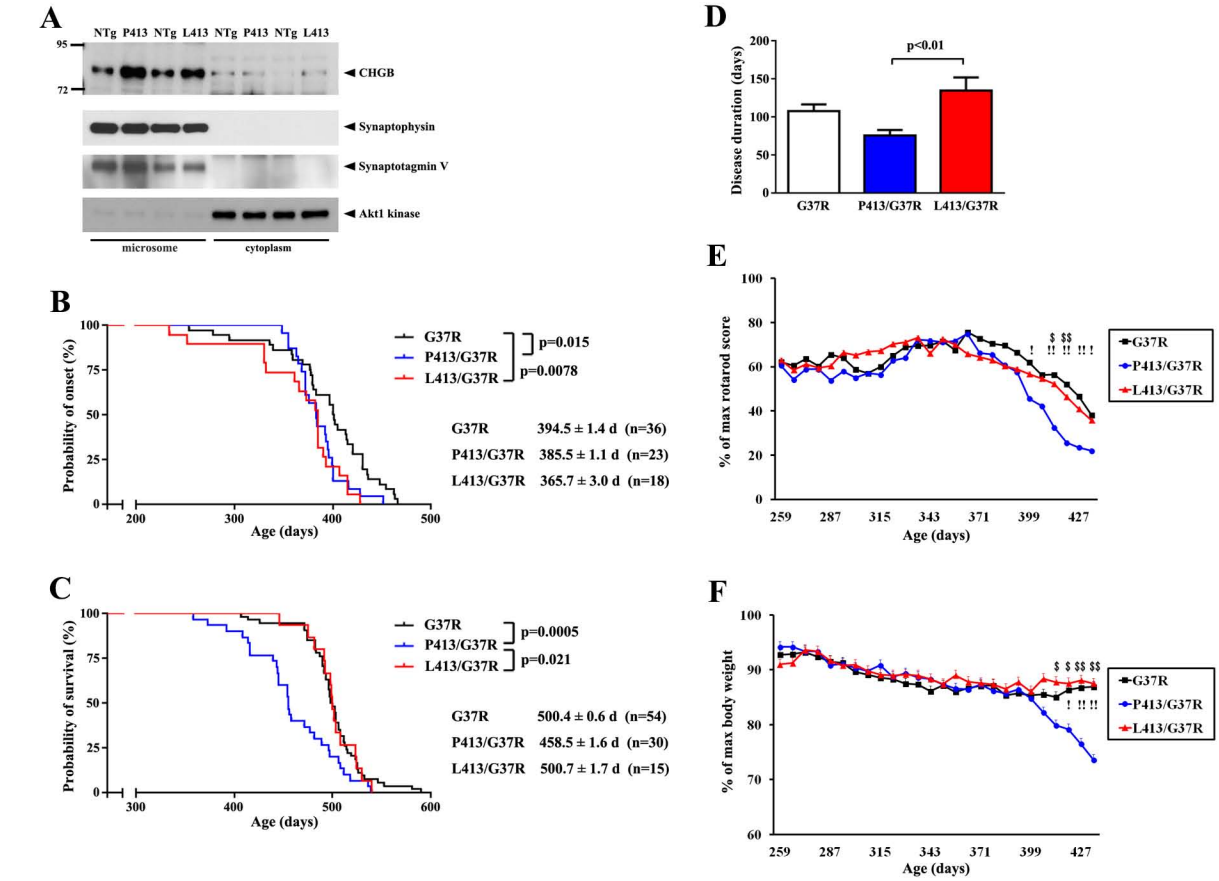
A
NTg P413 NTg L413 NTg P413 NTg L413
95
72
CHGB
Synaptophysin
Synaptotagmin V
Akt1 kinase
microsome
cytoplasm
B
Probability of onset (%)
Age (days)
G37R
P413/G37R
L413/G37R
p=0.015
p=0.0078
G37R 394.5 ± 1.4 d (n=36)
P413/G37R 385.5 ± 1.1 d (n=23)
L413/G37R 365.7 ± 3.0 d (n=18)
C
Probability of survival (%)
Age (days)
G37R
P413/G37R
L413/G37R
p=0.0005
p=0.021
G37R 500.4 ± 0.6 d (n=54)
P413/G37R 458.5 ± 1.6 d (n=30)
L413/G37R 500.7 ± 1.7 d (n=15)
D
Disease duration (days)
p<0.01
G37R
P413/G37R
L413/G37R
E
% of max rotarod score
Age (days)
G37R
P413/G37R
L413/G37R
F
% of max body weight
Age (days)
G37R
P413/G37R
L413/G37R

Fig S4

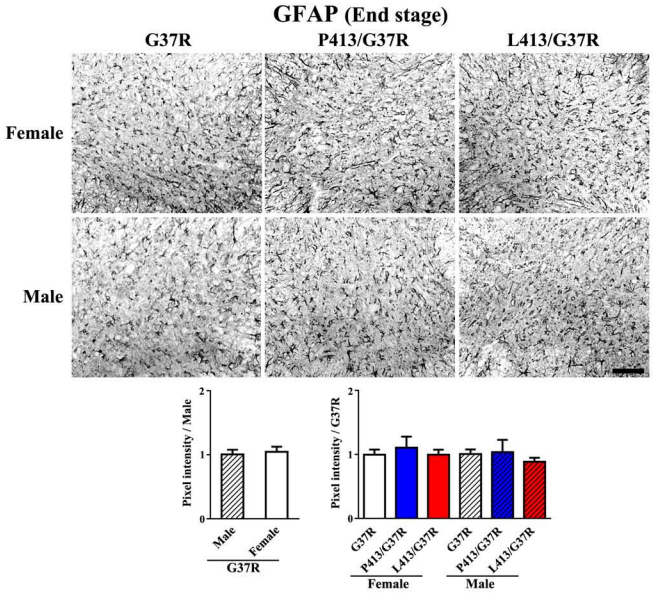
GFAP (End stage)
G37R
P413/G37R
L413/G37R
Female
Male
Pixel intensity / Male
2
1
0
Male
Female
G37R
Pixel intensity / G37R
2
1
0
G37R
P413/G37R
L413/G37R
G37R
P413/G37R
L413/G37R
Female
Male

Fig S5

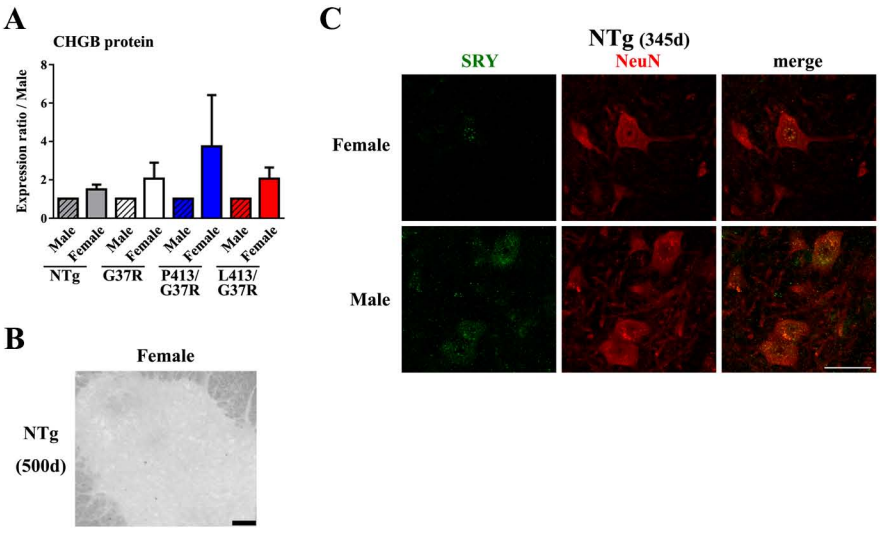
A
CHGB protein
Expression ratio / Male
8
6
4
2
0
Male
Female
NTg
G37R
P413/ G37R
L413/ G37R
B
Female
NTg
(500d)
C
NTg (345d)
SRY
NeuN
merge
Female
Male

Table S1. Non-Mendelian transmission of CHGB^{L413} transgene in female mice

The frequency of P413 or L413-hCHGB in Tg mice

	Variant frequency (%)		
	Female	Male	P-value
P413	78/160 (48.8)	88/166 (53.0)	0.44
L413	29/78 (37.2)	40/80 (50.0)	0.10

Table S2. Clinical details of study population of Japanese, French Canadians and French ALS

	Japanese	French Canadians and French
Total		
Number of individuals	**194**	**289**
Mean age of onset years (range)	**64 (24-87)**	**58 (23-82)**
Females		
Number of individuals	**66**	**113**
Mean age of onset years (range)	**66 (38-87)**	**57 (31-81)**
Males		
Number of individuals	**128**	**176**
Mean age of onset years (range)	**62 (24-83)**	**56 (23-82)**

Table S3. Homology of HMG box region in SRY between human and mouse

		HMG box region of SRY
human	(59-130)	rvkrpmnafivwsrdqrrkmalenprmrnseiskqlgyqwkmlteaekwpffqeaqklqamhrekypnykyr
mouse	(4-74)	hvkrpmnafmvwsrgerhklaqqnpsmqnteiskqlgcrwkslteaekrpffqeaqrlktlhrekypnyky

Table S4. List of primers used for genotyping hCHGB mice, quantitative real time RT-PCR and probes used for *in situ* hybridization

	Forward	Reverse
Genotyping hCHGB Tg mice		
P413	**5'agagaggggccttgagc3'**	**5'ctttagtgtcctgcaggtctc3'**
L413	**5'aacgtcagcatggccagtttag3'**	**5'gagggtcgtagtatgggttgatgaaca3'**
Quantitative real time RT-PCR		
hCHGB	**5'gatgaggaggacaagagaaactac3'**	**5'agctctttccacgcaccttgt3'**
Probes for *in situ* hybridization		
hCHGB	**5'aggagaagacacatagccgaga3'**	**5'taatacgactcactataggggttcaaggtcagctcattttcc3'**